Journal of Applied Polymer Science

Poly(butylene succinate-co-butylene adipate)/polyethylene oxide blends for controlled release materials: A morphological study

Amandine Cottaz, Fadi Khalil, Sophie Galland, Fouzia Jbilou, Isabelle Adt, Pascal Degraeve, Catherine Joly

Laboratoire de Bioingenierie et Dynamique Microbienne aux Interfaces Alimentaires (BioDyMIA, EA 3733, Universite de Lyon, Universite Claude Bernard Lyon 1 - ISARA Lyon, Technopole Alimentec, IUT Lyon 1 site de Bourg en Bresse, Rue Henri de Boissieu F-01000, Bourg en Bresse, France

Correspondence to: C. Joly (E-mail: catherine.joly@univ-lyon1.fr)

ABSTRACT: Varying the formulation and processing conditions of polymer blends allows the design of materials with a large range of morphologies. Active materials embedding active compounds in a devoted phase are promising applications of such blends, offering possible various transport properties. In this study, 13 poly(butylene succinate-co-butylene adipate) (PBSA)/polyethylene oxide (PEO) blends were extruded in a slit die. Their morphologies were characterized by water extraction (selective PEO dissolution), FTIR spectroscopy, and differential scanning calorimetry. Transport properties were assessed by water vapor permeation and fluorescein release as model migrant. Indeed, the desorption in water of fluorescein (previously entrapped in PEO) was monitored to preliminary investigate the release properties of these materials: two morphologies were obtained (i) pseudo multilayer films made of PEO-rich layer/PBSA-rich layer/PEO-rich layer and (ii) PEO nodules dispersed in the PBSA-rich matrix for the highest PBSA contents. The first systems were erodible ones with an uncontrolled fast delivery by PEO dissolution whereas the second ones showed a controlled release by permeation through the PBSA matrix from PEO nodules. © 2015 Wiley Periodicals, Inc. J. Appl. Polym. Sci. **2016**, *133*, 42874.

KEYWORDS: blends; films; morphology; packaging; structure–property relations

Received 29 March 2015; accepted 24 August 2015

DOI: 10.1002/app.42874

INTRODUCTION

To improve the quality of packaged foods and/or to extend their shelf life, active food contact materials, embedding active species, can be designed to absorb or release relevant substances. Amongst these active systems, antimicrobial materials allow the release of antimicrobial molecules onto surfaces of perishable foods to control undesirable microorganisms during their shelf life period.[1] However, although announced since the 1990s, development and commercialization of such packagings in European Union, are still hampered for many reasons such as: (i) *their processability*: the strategies used to incorporate active agents are limited by their thermal stability and are often incompatible with conventional plastic manufacturing conditions (for usual food grade plastics);[2] (ii) *their efficiency*: a release which is more or less well-controlled and their *antimicrobial activity loss* during storage as well as during the contact with foods;[3] (iii) *their cost* which is always higher than for a conventional "passive" packaging[4]; and (iv) for the *regulatory issues*.[5]

Most of the antimicrobial agents require devoted matrices or systems to be efficiently incorporated and then released.[6] As most of them are water soluble, these agents often require a polar matrix to be well solubilized before migration into the foodstuffs. However, most of the manufactured plastics used as food contact materials (for direct contact) are non-polar (polyethylene or polypropylene) or semi-polar ones (i.e., polyethylene terephthalate). Furthermore, these polymers require high temperatures to be converted into packaging which has been often reported not to be relevant with respect to the thermal stability of natural antimicrobial food preservatives.[7–9] This situation explains why most of the active packagings which are studied are polar ones mainly based on polysaccharides, proteins, polyols and derivatives.[10–15] However, their use is very limited as bulky materials mainly because of their high cost, high sensitivity to the ambient relative humidity modulating drastically their properties and because of the challenging routes to be conceived for their industrial processing.

To overcome such bottlenecks, research in pharmacy devoted to drug controlled release has promoted new systems based on immiscible polymers blends.[16,17] These systems could also be promising as active materials or coatings.[18] Indeed, varying both composition and processing conditions of polymer blends

allows the design of materials with a large range of morphologies associated to specific release properties. Blends of two immiscible or partially miscible polymers are often prepared to make biphasic materials with evolving morphologies: matrix-dispersed particle structures, matrix–fiber structures, lamellar structures or co-continuous structures.[19] The blends become active materials when active agents are incorporated into a relevant phase (i.e., the polymeric phase in which the active agent is soluble) before being mixed with the second polymer by plastic compounding.[18]

In the present study, the transport properties of films made of polyethylene oxide (PEO)/PBSA blends were investigated as a function of the material morphology. The choice of PEO and PBSA will allow the melt blending below 100°C, which is favorable to preserve a large panel of active agents from thermal degradation[20] for further studies. Moreover, PEO is a biocompatible, biodegradable and water soluble polymer. These specific features make it applicable also for drug delivery purposes. PBSA was chosen for its thermal properties located in between those of polyethylene and polypropylene. PBSA is also able to balance the weaknesses and drawbacks of PEO, which properties change with the hydration rate. The transport properties were assessed by water vapor permeation and a model migrant (fluorescein), [21] which mainly diffuse through the PEO phase and from PEO phase, respectively. Water was selected to quickly probe the polar PEO phase, and Fluorescein sodium salt was chosen as a water soluble molecule, easily detected, and stable during extrusion with an average molecular weight compared to food preservatives. It is not a good model for natural antimicrobials but a model for the study of the transport properties as a function of the blend formulation.

MATERIALS AND METHODS

The materials selected for the preparation of polymer blend films were a commercial poly(ethylene oxide) (PEO) powder with a number-average molecular weight M_n of 200,000 g mol^{-1} (Sigma Aldrich, Saint Quentin Fallavier, France) and pellets of PBSA (statistic copolyester with 80% of succinic acid [22]) was purchased from NaturePlast (PBE 001 reference, Caen, France). For fluorescein migration studies, PEO was formulated with fluorescein sodium salt (Sigma Aldrich, Saint Quentin Fallavier, France) as described below.

Preparation of PBSA/labeled-PEO Blends

Preparation of PEO Pellets Labeled with Fluorescein. PEO powder (2 kg), previously equilibrated at 50% RH and 23°C until constant weight (i.e., for one week), was stirred in a blender (Kenwood, KM286 Prospero, France) during the progressive addition of a fluorescein sodium salt aqueous solution (320 mL) (50 ppm/PEO (wt/wt dry basis)). The wetted mass was then homogenized for 5 min in the mixer. The wet mass was immediately extruded using a three-zone single-screw extruder (Rheoscam, Scamex, Crosne, France). The three zones of the extruder were heated at 80°C and the rotation speed was set at 100 rpm. The screw of the extruder had a length of 220 mm, with a length/diameter ratio of 11 (die diameter 2 mm). The strands issued from the first run were pelletized with a pelletizer (Pelletizer knives model, Scamex, Crosne, France) and equilibrated at 50% RH and 23°C before use.

PBSA/PEO Extrusion. Various PBSA/fluorescein-containing PEO blends (0, 10, 20, 30, 35, 40, 45, 50, 55, 60, 65, 70, 80, 90, and 100% PBSA) were prepared by mixing PBSA and PEO pellets.

The blends were denoted as follows: PBSA10 means that the blend contained 10% of PBSA and 90% of PEO.

Homogeneous blends were prepared with the same Scamex extruder equipped with a three-zone Scamex double-screw module. The three zones were heated at 90°C. Once pelletized (with a Scamex pelletizer), pellets were re-extruded with a four-zone single-screw extruder (Scamex). The four zones were heated at 90°C. The extruder was equipped with a slit die (die width 5 cm) followed by a three-roll calendaring system to prepare extruded films. The screw rotation speed was set at 50 rpm which gave an approximate residence time of ~55–60 s. The rotation speed of the calender was 30 rpm for a typical film thickness of 220 ± 10 μm.

Characterization of PBSA/PEO Films

Differential Scanning Calorimetry (DSC). The thermal properties of PBSA/PEO blends were determined by differential scanning calorimetry. DSC analyses were performed with a DSC Q20 apparatus (TA Instruments, Guyancourt, France). Ten milligrams of each film were weighted directly in appropriate pans sealed hermetically. Samples were first heated from 30 to 150°C with a heating rate of 10°C min^{-1}, before being cooled to 30°C at 10°C min^{-1} and heated again for a second run also undergone from 30 to 150°C at 10°C min^{-1}. The melting temperature T_m was taken at the onset of the melting peak for both first and second runs. Relative (or normalized) melting enthalpies of PBSA and PEO in the blends were calculated from the areas of their melting peaks on the basis of the heats of fusion of pure polymers (determined by performing the same thermal analysis) and taking into account the proportion of each phase in the blends.

ATR-FTIR Spectroscopy. Mid-infrared spectra of PBSA films were recorded from 400 to 4000 cm^{-1} (4 cm^{-1} resolution, 24 scans) using a FTIR Alpha spectrometer (Bruker optics, Wissembourg, France) coupled to a Platinum ATR module (diamond ATR crystal, depth at 1000 cm^{-1}: 1.66 μm). A spectral classification based on raw spectra (full range) using a cluster analysis based on a hierarchical classification algorithm with the Opus Ident procedure (Opus 5.5 software, Bruker optics) was carried out.

Water Sorption Isotherms. Water sorption isotherms at 23°C for films with different compositions were performed gravimetrically using a microbalance (Q5000SA, TA Instruments, Guyancourt, France). The samples mass was about 5–6 mg. The samples were dried at 45°C (under dynamic dry nitrogen flux) until constant weight (variation< 0.005 wt % for 30 min) before being equilibrated at different relative humidities (0, 20, 40, 60, 75, 85, and 95% RH), (variation< 0.005 wt % for 30 min).

Blend Morphology Study

PEO extraction (by water) and microscopic observations were combined to investigate the blend morphology.

Selective Extraction of PEO by Water. Extraction of PEO phase by water allowed quantifying its continuity index as reported in the literature as a standard method.[19] Two grams of each formulation (pellets or films) was immersed in 250 mL of water at 20°C directly for pellets, enclosed in a woven wire cloth for films. After 24 h, the samples were dried during 24 h at 50°C. The extraction procedure was repeated three times. The continuity index of PEO was defined as the fraction of polymer that belongs to a continuous phase and was calculated with eq. (Eq. 1):

$$\%\ \text{continuity of } i = \frac{(\text{weight of } w\text{hole sample-weight of sample after extraction of } i)}{(\text{weight of } i\ )\text{in the sample before extraction}} \times 100 \qquad \text{(Eq. 1)}$$

Scanning Electron Microscopy (SEM) Observations. After extraction of PEO, samples were examined with a Hitachi S3000-N scanning electron microscope (Verrières-le-Buisson, France) at 5 kV accelerating voltage. The samples were fractured after immersion in liquid nitrogen and sputter-coated with gold. The sections were observed.

Water Vapor Transmission Rate (WVTR). Films (0, 10, 20, 30, 35, 40, 45, 50, 55, 60, 65, 70, 80, 90, and 100% PBSA, typical thickness around 220 ± 10 μm, preconditioned one week at 50% RH and 23°C) were each sealed on one aluminum foil mask, purchased from Labomoderne (Paris, France), leaving an uncovered film area of 3.14 cm^2. Araldite epoxy resin (Bostik, Courbevoie, France) was used to insure water and air tightness at the contact zones between the films and the foil masks. All actual exchange surfaces after deposition of epoxy resins recalculated by optical analysis were between 2 and 3 cm^2. Water vapor transmission rates (WVTR) were determined at 23°C for a partial pressure gradient equal to 50–75% RH. WVTR were measured by the "wet cup method" as the water vapor fluxes were high enough, placing the films over the top of a pre-made watertight metal cup. The cup contained a sodium chloride saturated aqueous solution and was placed in a climatic chamber (50% RH, 23°C). Theoretical permeability (P) of multilayered films (total thickness L) comprising three layers of different properties (P_i, l_i) sandwiched together was calculated with the following equation where l_i stands for the thickness of each layer:

$$L/P = l_1/P_1 + l_2/P_2 + l_3/P_3 \qquad \text{(Eq. 2)}$$

Desorption Kinetics of Fluorescein from Films to Water

Desorption kinetics of fluorescein from PEO phase of films to water was monitored with a spectrofluorometer (LS 55, Perkin Elmer, Courtaboeuf, France) at 23°C as a function of the film composition. Extruded films were molded to reduce their thicknesses to a constant value (70 ± 10 μm) using a thin film making kit placed in a hydraulic press equipped with platens heated at 120°C (Specac, Eurolabo, Saint Chamond, France), a 4 ton pressure was applied for 20 s. Films were properly shaped as disks of 8 mm diameter. One disk was suspended from a needle passing through the cap cell before being immersed in 4 mL distilled water placed into disposable poly(methylmethacrylate) cells. All systems (cell + suspended film) were excited at 490 nm thanks to a four-position automatic cell changer. The emission was recorded every minute at 560 nm until equilibrium to avoid any saturation phenomenon and to have enough sensitivity at the beginning of desorption. Migration tests were replicated 4 times for each blend composition.

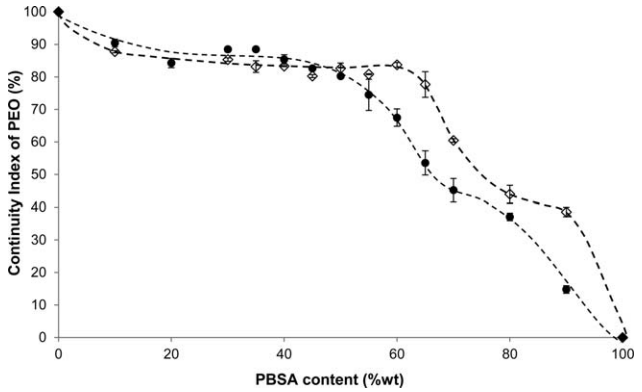

Figure 1. Continuity index of PEO in PBSA/PEO pellets (●) and films (◇) as a function of the PBSA content.

RESULTS AND DISCUSSION

Blend Morphology Study

The blend morphology was investigated thanks to the water extraction of PEO and SEM observations in order to investigate the relationships between the structure of films and the transport properties which could be used as active materials.

Selective Extraction of PEO. PEO being water soluble, the blend morphology was investigated after water extraction in order to determine the percentage of PEO able to be extracted from the blends (i.e., PEO available to water). In the literature,[19,23] this percentage is defined as the continuity index (CI) of the extracted phase. In Figure 1, both pellets and films thereof have been extracted with water for all compositions and the CIs were displayed as a function of the blend composition. Both curves showed the same trend: a decrease in PEO continuity index from 100 (fully removable) to 0% (entrapped in PBSA). Meanwhile, when the PBSA content increased, a pseudo plateau was noticeable between 10 and 50 wt % PBSA for pellets, and between 10 and 65 wt % PBSA for films. This pseudo plateau means that an important part of the PEO phases in this region (from 80 to 90%) was available for water dissolution probably because belonging to the continuous phase, thus removable. Reciprocally, an amount of 10 to 20 wt % of PEO was irreversibly entrapped by PBSA in that plateau region. In details, for the first experimental point of the plateau (PBSA 10), PBSA (10% wt) is surprisingly able to entrap nearly its own mass of PEO (10% wt). This surprising result was also observed qualitatively as films kept their integrity as thinner but fragile films when immersed in water. At those high PEO percentages, the CI values were expected to be close to 100% as always observed in the literature for other blends.[23] Here, the

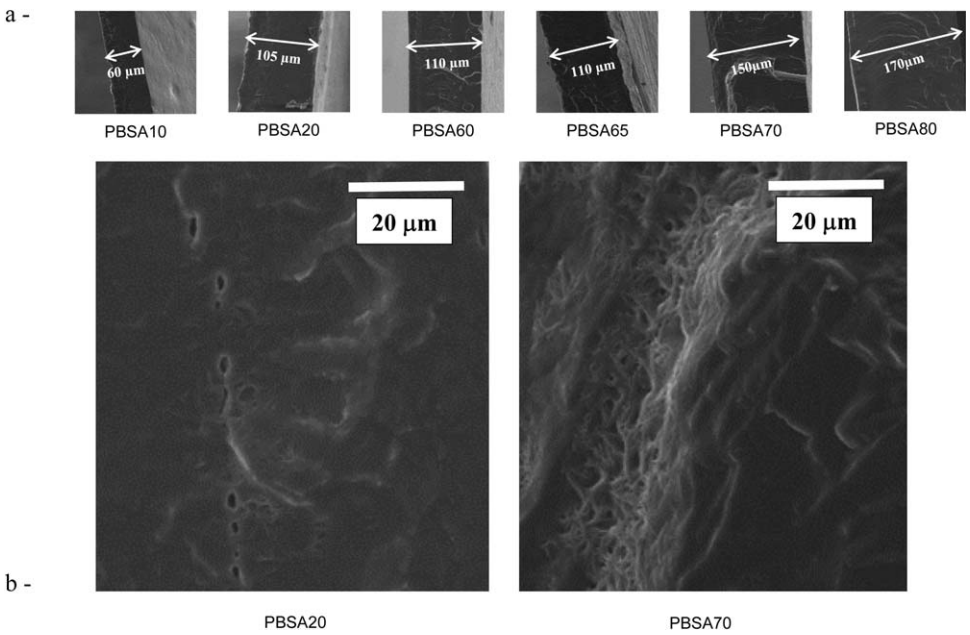

Figure 2. SEM observations of cryofractured films after PEO extraction by water (same magnification). (a) Thicknesses of the inner PBSA-rich layers (PBSA 90 not shown as its thickness was unchanged), (b) magnification of the cross-section of PBSA 20 and PBSA 70 showing small holes.

PBSA phase had a preserved structure after processing and water immersion and was still able to partially entrap the second phase (PEO): water was likely not able to penetrate into PBSA crystallites to reach and solubilize entrapped PEO. This phenomenon has already been reported with crystalline/crystalline blends such as PBS (polybutylene succinate)/PEO. Authors explained this property as a PEO segregation within the interlamellar regions of PBS.[24] In that way, the originality of this study compared to literature was to quantify the amount of PEO (10 to 20% wt) sufficiently well entrapped inside PBSA crystallites or co-crystallites not to be removed by a simple dissolution in water (Figure 1).

After the pseudo plateau, pellets and films acted differently: the PEO continuity indexes declined faster until PBSA 65 for films but sooner (from PBSA55) for pellets showing both an inflexion point at PBS70. PEO was more extractable from films as their morphology can be somehow modified by the mechanical stress induced by the slit die followed by the calendering process. A more pronounced shoulder (inflexion point) was observed for films: for example, for PBSA20 up to 40–50% of PEO were still extractable against only about 15% of PEO for pellets. As a conclusion, pellets and films seemed to show nearly the same behavior except for the high PBSA contents, which could probably be due to the different rheology of polymers at molten state.[25]

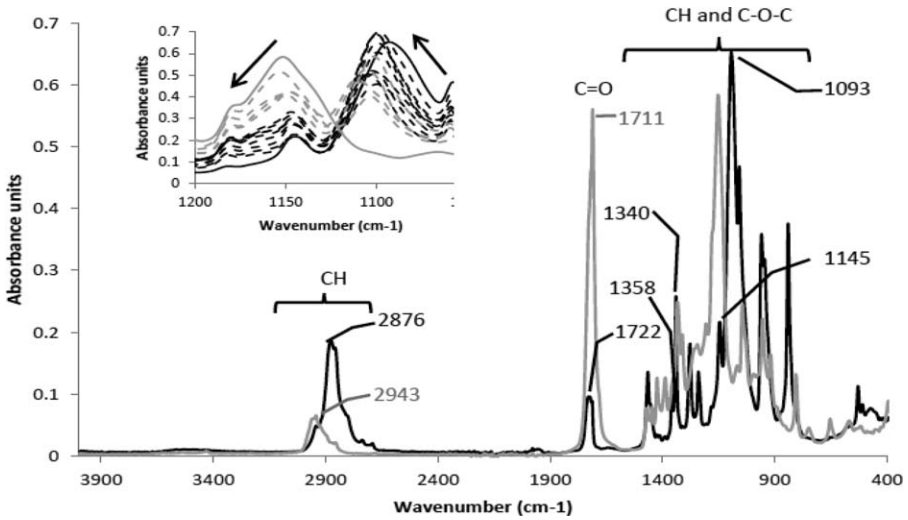

Figure 3. FTIR spectra of neat PEO (black line and black peak labeling) and neat PBSA films (gray line and gray peak labeling). The inset corresponds to a focus (1250 to 1050 cm^{-1} wavenumbers area) for films made with 10 to 60% wt PBSA (black dotted lines) and for films made with 65 to 90% wt (gray dotted lines).

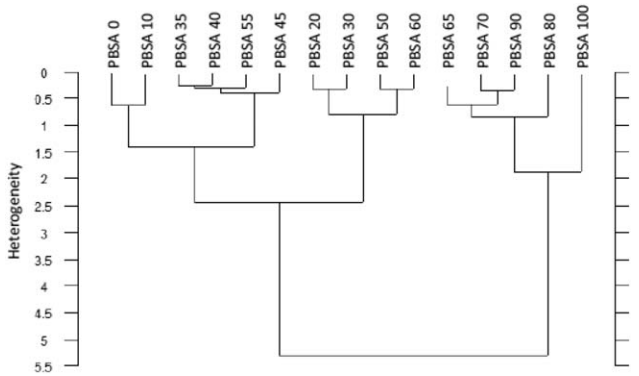

Figure 4. Hierarchical clustering of the 15 PBSA/PEO films based on ATR-FTIR spectra analysis (full spectral range 400–4000 cm^{-1}).

SEM Observations of Films. SEM observations have been performed after [Figure 2(a,b)] the water extraction of films in order to precise the multiphasic structure of the systems. Before extraction, no peculiar morphologies were observed as the phase contrast between the both polymers was not sufficient enough. This observation was consistent with the literature regarding PEO/PBS blends[26,27] which suggests the presence of partially miscible systems or of nodules of very small size possibly obtained following the twin screw extrusion (data not shown).

After the PEO removal, the film integrity was surprisingly preserved despite of the water immersion but their thicknesses were reduced: the PBSA formed a continuous film which resisted to the water immersion from the early PBSA percentages. The new thicknesses of films (originally 220 μm) decreased to approximately 60 μm for PBSA 10, 105–110 μm for PBSA 20 to 65, 150 μm for PBSA 70 and reached 170 μm for PBSA 80 before being nearly unchanged for PBSA 90 [Figure 2(a)]. From these results, it was now possible to conclude to a multilayered structure made of an inner layer of a PBSA-rich phase [Figure 2(a)] surrounded by skin layers made of a PEO-rich phase. Belard *et al.*[25] also obtained pseudo-multilayered systems for PCL (polycaprolactone)/PLS blends aiming at surface property modifications of materials. The observations of film cross-sections showed small holes in the PBSA-rich layer, displayed in Figure 2(b) for PBSA 20 and 70. From literature, it is reported in polymer blends that these holes would be adjustable via process control and would also mechanically connect adjacent layers to prevent delamination.[28,29] These morphologies are known as selective permeable morphology.[29]

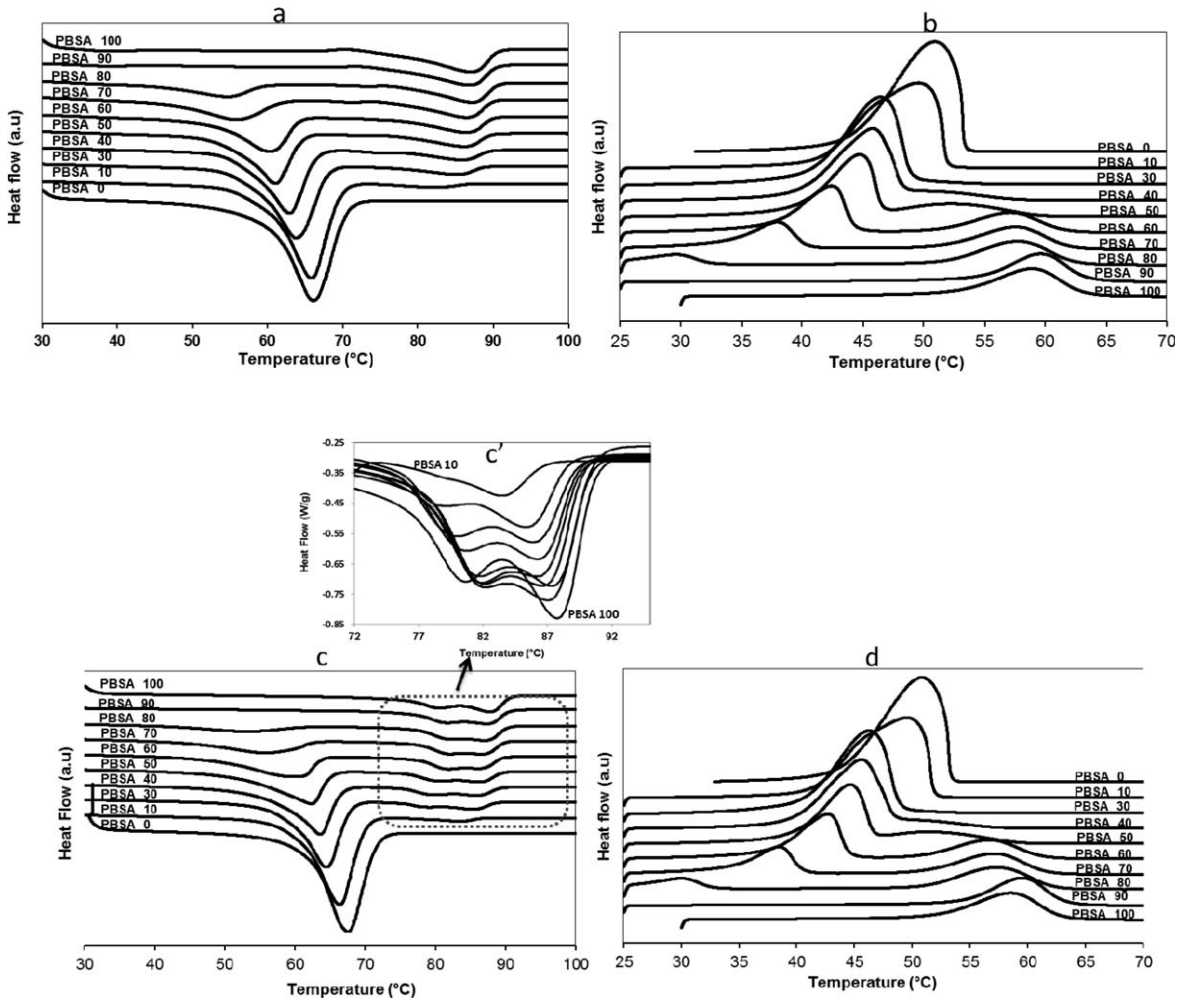

Figure 5. DSC thermograms of PEO/PBSA blends—5(a,b): first run (heating and cooling ramps), 5(c,d): second run. (a.u.: arbitrary units).

Table I. Thermal Properties (T_m and T_c) and Normalized Crystallinity Rates of PBSA/PEO Blends

	PEO							PBSA					
	First run				Second run			First run				Second run	
Sample	*Tm* (°C)	Melting enthalpy ($J.g^{-1}$)	Normalized melting enthalpy (%)	T_c (°C)	T_m (°C)	Melting enthalpy ($J.g^{-1}$)	Normalized melting enthalpy (%)	T_m (°C)	Melting enthalpy ($J.g^{-1}$)	Normalized melting enthalpy (%)	T_c (°C)	Melting enthalpy ($J.g^{-1}$)	Normalized melting enthalpy (%)
PBSA0	66	142	100	51	68	140	100	/	/	/	/	/	/
PBSA10	66	133	104	50	66	117	93	83	4	112	/	4	92
PBSA30	64	106	106	46	64	86	88	85	11	100	/	13	92
PBSA35	63	98	106	46	64	78	85	86	12	93	/	15	93
PBSA40	63	87	102	46	64	69	82	86	12	81	/	18	96
PBSA45	62	77	98	45	63	62	80	86	13	78	51	20	96
PBSA50	61	73	103	45	62	61	88	86	16	83	53	21	91
PBSA55	60	64	100	44	61	51	81	86	18	85	53	23	89
PBSA60	60	60	105	42	60	45	81	87	21	91	57	24	86
PBSA65	59	53	106	40	57	41	84	87	24	97	58	26	86
PBSA70	56	44	102	38	56	33	79	87	23	89	58	27	83
PBSA80	54	30	104	30	53	16	58	87	24	79	58	29	80
PBSA90	38	2	12	/	/	/	/	87	31	91	60	37	89
PBSA100	/	/	/	/	/	/	/	87	38	100	59	46	100

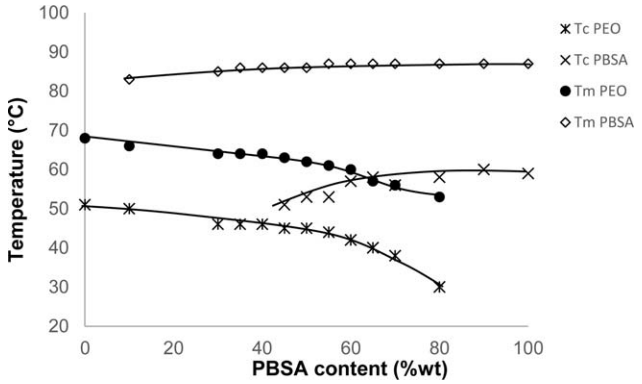

Figure 6. Melting and crystallization temperatures of PBSA and PEO as a function of the PBSA content in PEO/PBSA blends.

Blend Surface Analysis by ATR- FTIR. ATR-FTIR analyses were performed to investigate the surface properties of blends. In Figure 3, spectra of films made of neat PEO and PBSA were analyzed and taken as references according to Hexig *et al.*[30–32] PEO FTIR spectrum presented a typical band centered at 2876 cm^{-1} corresponding to the CH (from CH_2 groups) stretching region. Such a peak was also present in PBSA FTIR spectrum but at a 2943 cm^{-1} wavenumber and with a weaker absorbance. The main specific bands for PBSA films were attributed to the carbonyl (C=O) vibration region, centered at 1711 cm^{-1}. PEO and PBSA films spectra presented both some bands in the 900 to 1500 cm^{-1} region, mainly assigned to CH (from CH_2 groups) stretching and deformation. A band centered at 1093 cm^{-1} of PEO film spectrum could be attributed to the C-O-C elongation (ether function). From raw full spectra of all PBSA/PEO films, a hierarchical classification was performed in order to group all the films on the base of their "surface" structural characteristics (the penetration depth of IR beam into the sample was about 2 μm). The dendogram obtained from cluster analysis (Figure 4) shows a clear separation in two groups: the first cluster includes films containing less than 65%wt of PBSA whereas the second one gathers films containing more than 65% wt of PBSA. These results highlighted that the "surface" composition of films made from PEO/PBSA blends containing from 10 to 60% wt PBSA was more similar to PEO. This is consistent with previous proposition that the PEO phase could be continuous or partially continuous in the superficial zone of these films, while the superficial composition of films made from blends containing from 65 to 90% wt PBSA would be similar to PBSA (PBSA partial/total continuity). The two clusters are obviously well marked especially for the peak at 1150 cm^{-1} (inset, Figure 4) and molecular interactions occurred between both phases as significant peak shifts are noticeable[33] (see arrows in the inset).

Analysis of ATR-FTIR spectra of films was consistent with the existence of multilayered (or more exactly pseudo multilayered) films made from 0 to 65% PBSA (Figure 4) as proposed following selective extraction of PEO by water and SEM observations. When PBSA proportion in blends exceeded 65% wt. (Figure 4), films surfaces would be mainly based on PBSA (as PBSA-rich skin layer) which would result from a phase inversion phenomenon.

Crystalline Morphology of Blends

Differential scanning calorimetry (DSC) thermograms (Figure 5, Table I) were recorded and analyzed for nearly all films focusing on PEO and PBSA melting or crystallization temperatures (T_m and T_c) and corresponding melting enthalpies (ΔH_m). These analyses were performed in order to investigate the crystalline morphology of blends to check whether the multilayered structure or any supplementary thermal event such as hot-pressing above T_m applied to obtain thinner films (for dimensioning of release systems) can modify any specific thermal properties. Two runs made of both heating and cooling ramps were performed. The first run was useful for films used directly after preparation (i.e., blend properties or water transport properties) and the second run for films which were pressed at molten state before being used (i.e., for fluorescein desorption in water experiments). Table I gathers collected values (T_m, Tc, enthalpies) for PEO and PBSA when measurable and for neat PBSA. As previously reported,[34–36] two melting peaks are noticeable for the second heating ramp. These authors reported such usual multiple events for thermoplastic PBSA because of crystal structure modification during the heating scan and/or the presence of melting, re-crystallization, and re-melting phenomena.

When the PBSA proportion in blends increased, both melting and crystallization temperatures of PEO decreased progressively and significantly from 66 to 38°C and from 50 to 30°C (Figure 6), for the first and second run, respectively. PBSA prevented the PEO phase from crystallization especially at the highest PBSA contents. From Figure 5, it is to be noted that PEO incorporated in PBSA90 (i.e., 10% wt of the whole material) is nearly totally amorphous as no endothermic peak was observed, especially during the second run. However, the normalized melting enthalpies of PEO blended with PBSA were rather unchanged

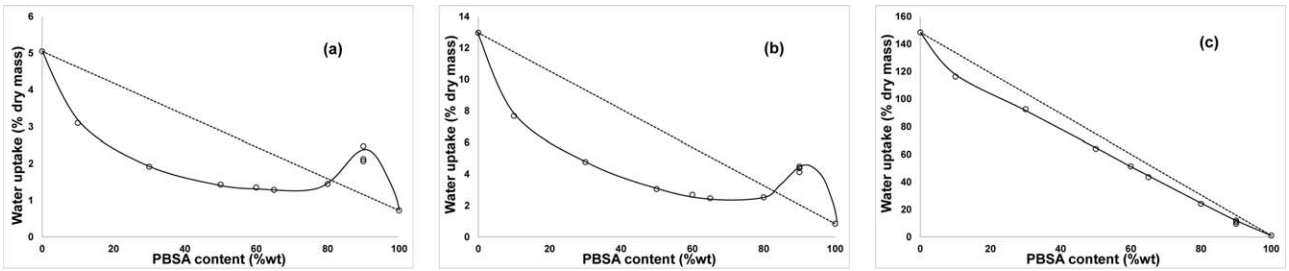

Figure 7. Experimental water uptake of films at 75% RH (a); 85% RH (b); 90% RH (c) and 23°C compared to theoretical water uptake (dotted line) calculated from the mixing law.

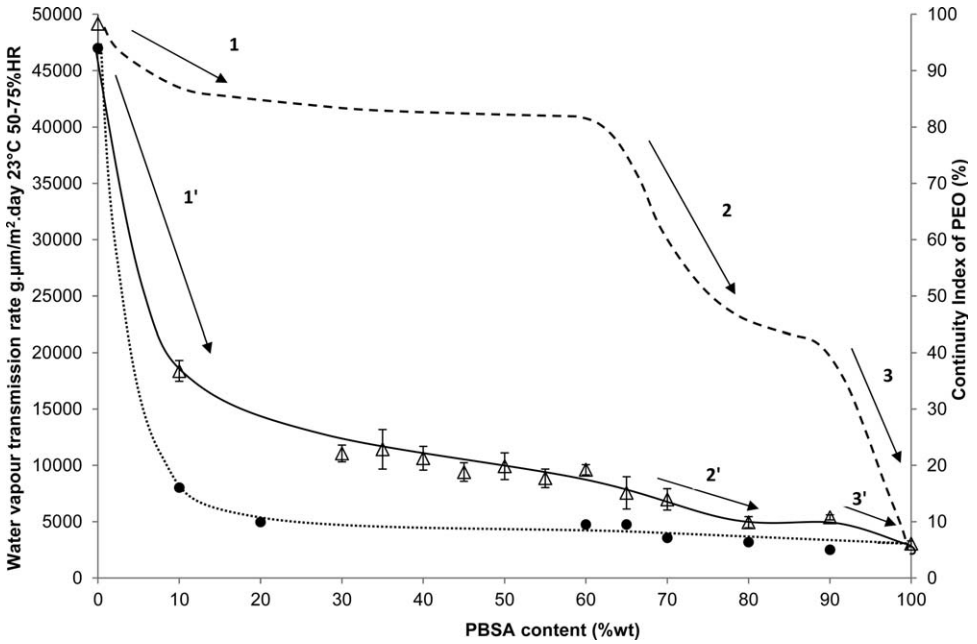

Figure 8. Water vapor transmission rate as a function of the blend composition (△) and theoretical fluxes for a relative humidity gradient of 75/50% through multilayered films at steady state (●). PEO continuity index curve from Figure 1 (—) is proposed for correlation purposes.

whatever the PBSA content except here again for the highest PBSA rates PBSA90 for first run and PBSA 80 for the second run [i.e., the normalized enthalpies decreased from 100% to only 12% (PBSA90, run 1) or 58 (PBSA 80, run 2) until 0% (PBSA90, run 2)].

Concerning PBSA, its melting temperatures were rather constant whatever the PEO percentage in blend even if the events were less scattered for the second run (but with double peaks). The crystallization temperatures increased slightly from 51 to 59°C (Figure 6) but this was only observed with half of the blends (from PBSA50 to PBSA100) since when PBSA proportion in the blends was less than 50%, the PBSA crystallization exotherms were masked by the more pronounced PEO ones.

The melting enthalpies of PBSA corresponding to the first run were obviously more scattered than for the second run where the normalized melting enthalpies were varying from 90% until PBSA80 before to increase up to 100%. For all blends below PBSA90, 10% of PBSA would be almost amorphous due to the PEO presence.

Water Sorption Isotherms of PEO/PBSA Blends and Water Vapor Permeation

Water Sorption Isotherms. Figure 7 displays the film water uptake at equilibrium at 75% RH for films made from blends. The water uptake decreased when the PBSA content increased as expected considering the hydration rate of the neat components. PEO was responsible of the main water sorption as neat PEO sorbed 5% wt of water molecules against 0.7% wt for PBSA at 75% RH. The experimental data were not in good agreement with the theoretical water uptake: the blends sorbed much less water than theoretically expected. PEO sorption sites were surprisingly much less available for water in the blends except for PBSA 90. At this high PBSA percentage, the embedded PEO was nearly amorphous and could thus sorb more water molecules than expected from the mixing law due to its more open structure. At 95% RH, the discrepancy between theoretical and experimental water sorption was more limited, likely because materials were swollen (at this RH, PEO sorbed up to 148% wt of water) and then modified for PEO by free water since water may have exceeded the quantity of water specific sorption sites on PEO chains. Blend characterization by water vapor permeation study

Water Vapor Permeation. The water vapor transmission rates (WVTR) of films has been performed as water molecules are able to investigate selectively (at a microscopic scale) the polar PEO phase:[18] the water permeability coefficients for neat PEO and PBSA are drastically different (i.e., 16 times lower for PBSA). For this experience, an increment of water vapor partial pressure has been chosen (75%–50% RH) in order to moderately hydrate the membranes (avoiding water dissolution or swelling of PEO). This hydration level corresponds to the water sorption isotherms performed in the former paragraph.

In Figure 8, the water vapor transmission rates at steady state were displayed as well as the PEO continuity indexes from Figure 1 and theoretical permeations based on the overall permeability calculated from eq. (Eq. 2) for multilayered films. As expected, the water permeability decreased when PBSA content increased in the blend. From Figure 8, it is clear that the changes in both the water transport and the PEO continuity index are well correlated as a function of the film composition presenting both three decreasing stages, with contrasting amplitudes (a high decrease in WVTR corresponds to a lower one in CI and reciprocally). These three trends were displayed by arrows. The first arrow (1), when 20% to 30% of PBSA were added to PEO, corresponded to the most important WVTR decrease (from 45,000 to 10,000 g μm/m^2 day) linked to the

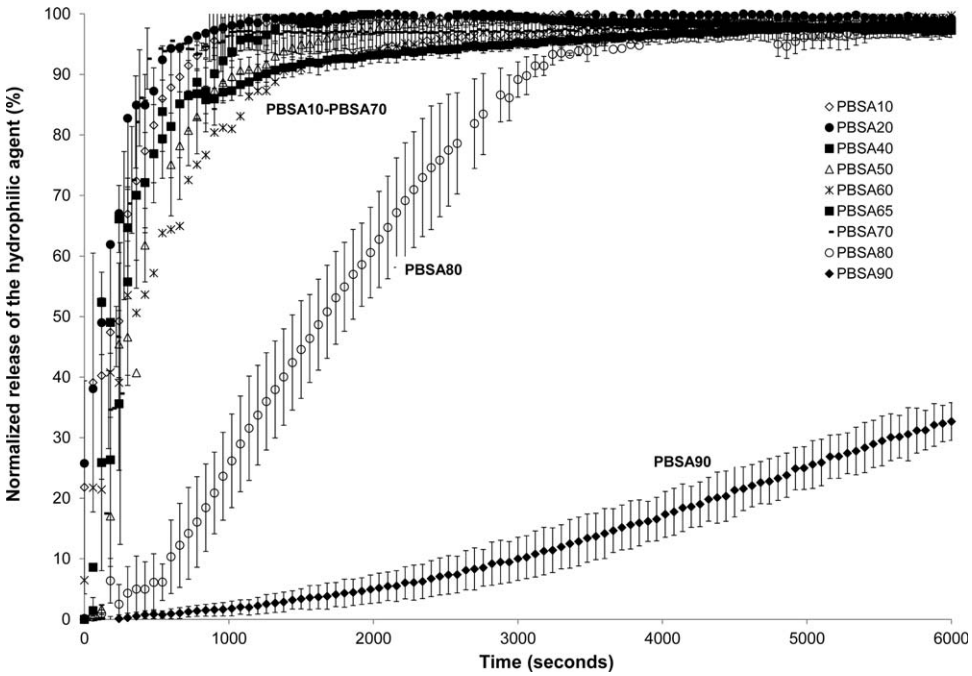

Figure 9. Fluorescein desorption kinetics from PBSA/PEO blends into water as a function of the blend composition. The intensity ratio corresponds to the percentage of released fluorescein. Each point and error bar correspond to the mean and standard deviation of three independent experiments for a given PBSA content.

water sorption reduction previously observed (Figure 7). Following this first decrease of WVTR, a pseudo plateau region between 20% wt and 60% wt PBSA was observed. It is noteworthy that it also corresponds to the plateau previously observed for PEO continuity index. Then, a second but lower decrease in WVTR occurred (from 12,000 to 7000 g μm/m^2 day) and followed by a third much smaller one. The first huge decrease corresponds to the elaboration of the inner layer of PBSA. Here, PBSA acts as a water barrier for the laminate (compared to PEO) even if this inner layer is not a neat PBSA one as already discussed (Figure 2). Indeed, the permeability values should be lower in the case of a neat PBSA layer [see the theoretical values calculated from eq. (Eq. 2)] taking into account the thicknesses of every layer on the basis of Figure 2(a). After the plateau, diffusion began to occur mainly through PBSA as the phase inversion phenomenon began above a 65% wt PBSA (as already stated from ATR-IRTF results). This likely explains the second decrease. The last decrease corresponds to the gradual disappearance of PEO diffusion paths to attain the WVTR of neat PBSA.

Kinetics of Release of Fluorescein in Water

To investigate if the film morphology can control not only the water diffusion but also the release of molecules of higher molecular weight, fluorescein sodium salt was chosen as a model migrant for its easy detection when released from PEO phase into water. From Figure 9, two different kinetics of fluorescein desorption profiles could be distinguished: (i) for films made from blends containing from 10 to 70% wt PBSA, fluorescein desorption is uncontrolled and due to PEO dissolution in water. It was meanwhile unexpected that for PBSA65 (i.e., after the phase inversion), or 70 no significant kinetic effect was observed. This could be due either to the reprocessing of materials performed to obtain thinner films for the dimensioning of the releases (quicker release) which could have delayed the inversion phase region to the higher PBSA percentages or to the immersion in water: this could have drastically swollen the films opening thus new diffusion paths despite of the CI curve evolution. (ii) For the second group (gathering PBSA80 and PBSA 90), the transport is well controlled by the morphology. The kinetics looked like permeation curves including time-lag, and release is proportional to time at the steady state (constant delivery rate). This time-lag was likely related to the transport of fluorescein from the PEO phase acting as a reservoir through the "walls" of PBSA continuous phase.

CONCLUSION

In this study, PBSA/PEO was blended at molten state using usual plastic processing to avoid any use of solvent. The morphologies of the films were studied as a function of their composition. Two typical morphologies were obtained after extrusion-calendering: pseudo multilayer films (PEO-rich layer/PBSA-rich layer/PEO-rich layer) for higher PEO contents which was not expected and PEO nodules dispersed in the PBSA matrix. The first systems are erodible ones with a fast and uncontrolled delivery due to PEO dissolution. The delivery rate of the second ones is controlled by the morphology and constant: the release proceeds by permeation from PEO nodules-reservoir through the PBSA matrix. The ongoing experiments will now focus on parameters able to finely control the flux of actual active substances (food preservatives instead of fluorescein) to deliver by playing with parameters such the average molecular weight of polymer to modulate the erodibility of

systems (crystalline morphology) as well as the water activity of the receptor media (gel or model food).

ACKNOWLEDGMENTS

The authors would like to express their gratitude to Dergham Co. Ltd (Tartus, Syria) for financing the Ph. D. grant of Mr. Fadi Khalil. They also acknowledge PTI Alimentec (Innovative technological platform) (Bourg en Bresse, France) for access to Dynamic Vapor Sorption analysis equipment and Mr. Chedi Merhaben (engineer student, INSAT, Tunis, Tunisia) for his active participation to the laboratory work during his training period in the laboratory.

REFERENCES

1. Appendini, P.; Hotchkiss, J. H. *Innov. Food Sci. Emerg. Technol.* **2002**, *33*, 113.
2. Brody, A.; Strupinsky, E.; Kline, L. Active Packaging for food applications, *Technomic Publishing Co. Lancaster* **2001**, 175.
3. Gharsallaoui, A.; Joly, C.; Oulahal, N.; Degraeve, P. *Crit. Rev. Food Sci. Nutr.* (in press).
4. Dainelli, D.; Gontard, N.; Spyropoulos, D.; Zondervan-van den Beuken, E; Tobbak, P. *Trends Food Sci. Technol.* **2008**, *1919*, 103.
5. European Parliament and Council of the European Union, Materials and Articles Intented to Come into Contact with Food, Regulation CE no. 1935/2004, Commision of the European Communities, Active and Intelligent Materials and Articles Intended to Come into Contact with Food, CE no. 450/2009.
6. Sung, S. Y.; Sin, L. T.; Tee, T. T.; Bee, S. T.; Rahmat, A. R.; Rahman, W. W. W.; Tan, A. C.; Vikhraman, M. *Trends Food Sci. Technol.* **2013**, *3333*, 110.
7. Jbilou, F.; Galland, S.; Tellier, C.; Akkari, Z.; Roux, R.; Oulahal, N.; Dole, P.; Joly, C.; Degraeve, P. *Enzyme Microb. Technol.* **2014**, *6767*, 40.
8. Colak, B. Y.; Peynichou, P.; Galland, S.; Oulahal, N.; Assezat, G.; Prochazka, F.; Degraeve, P. *Ind. Crop. Prod.* **2015**, *72*, 142.
9. Han, J. H.; Floros, J. D. *Food Sci. Biotechnol.* **1999**, *88*, 11.
10. Karbowiak, T.; Gougeon, R.; Rigolet, S.; Delmotte, L.; Debeaufort, F.; Voilley, A. *Food Chem.* **2008**, *106106*, 1340.
11. Cuq, B.; Gontard, N.; Guilbert, S. *Cereal Chem.* **1998**, *7575*, 1.
12. Hotchkiss, J. H. *Addit. Contam.* **1997**, *1414*, 601.
13. Imran, M.; El-Fahmy, S.; Revol-Junelles, A. M.; Desobry, S. *Carbohydr. Polym.* **2010**, *8181*, 219.
14. Sebti, I.; Chollet, E.; Degraeve, P.; Noël, C.; Peyrol, E. *J. Agric. Food Chem.* **2007**, *5555*, 693.
15. Del Nobile, M. A.; Conte, A.; Buonocore, G. G.; Incoronato, A. L.; Massaro, A.; Panza, O. *J. Food Eng.* **2009**, *9393*, 1.
16. Siepmann, F.; Siepmann, J.; Walther, M.; MacRae, R. J.; Bodmeier, R. *J. Control. Release* **2008**, *125125*, 1.
17. Lyu, S. P.; Sparer, R.; Hobot, C.; Dang, K. *J. Control. Release* **2005**, *102102*, 679.
18. Khalil, F.; Galland, S.; Cottaz, A.; Joly, C.; Degraeve, P. *Carbohydr. Polym.* **2014**, *108108*, 272.
19. Pötschke, P., Paul, D. R. *J. Macromol. Sci. Polym.* **2003**, *C43*, 87.
20. Liu, L. S.; Jin, T. Z.; Coffin, D. R.; Hicks, K. B. *J. Agric. Food Chem.* **2009**, *5757*, 8392.
21. Leuenberger, H.; Bonny, J. D.; Kolb, M. *Int. J. Pharm.* **1995**, *115115*, 217.
22. Jbilou, F.; Joly, C.; Galland, S.; Belard, L.; Desjardin, V.; Bayard, R.; Dole, P.; Degraeve, P. *Polym. Test.* **2013**, *3232*, 1565.
23. Chaput, S.; Carrot, C.; Castro, M.; Prochazka, F. *Rheol. Acta* **2004**, *4343*, 417.
24. Wang, H.; Schultz, M. J.; Yan, S. *Polymer* **2007**, *4848*, 3530.
25. Belard, L.; Dole, P.; Averous, L. *Polym. Eng. Sci.* **2009**, *4949*, 1177.
26. Ikehara, T.; Hironori, K.; Zhaobin, Q. *Macromolecules* **2005**, *3838*, 5104.
27. Pengju, P.; Zhao, L.; Yang, J.; Inoue, Y. *Macromol. Mater. Eng.* **2013**, *298298*, 201.
28. Lacoste, A.; Schaich, K. M.; Zumbrunnen, D.; Yam, K. L. *Packag. Technol. Sci.* **2005**, *18*, 77.
29. Zumbrunnen, D. A.; Inamdar, S.; Kwon, O.; Verma, P. *Nano Lett.* **2002**, *2*, 1143.
30. Hexig, B.; Alata, H.; Asakawa, N.; Inoue, Y. *Adv. Funct. Mater.* **2005**, *15*, 1630.
31. Alcantar, N. A.; Aydil, E. S.; Israelachvili, J. N. *J Biomed. Mater. Res.* **2000**, *51*, 343.
32. Zhao, H.; Liu, Z.; Park, S.; Kim, S. H.; Kim, J. H.; Piao, L. *Bull. Korean Chem. Soc.* **2012**, *3333*, 1638.
33. Fang, Y.; Prashantha, K.; Soulestin, J.; Lacrampe, M. F.; Krawczak, P. *Carbohydr. Polym.* **2013**, *9191*, 253.
34. Wang, Y.; Bhattacharya, M.; Mano, J. F. *J. Polym. Sci. Part B: Polym. Phys.* **2005**, *4343*, 3077.
35. Yasuniwa, M.; Tsubakihara, S.; Satou, T.; Iura, K. *J. Polym. Sci. Part B: Polym. Phys.* **2005**, *4343*, 2039.
36. Ray, S.; Bandyopadhyay, J.; Bousmina, M. *Polym. Degrad. Stab.* **2007**, *92*, 802.